Noncircular CFRP bicycle's chainring. part I: static and low-velocity impact analysis

Zhorachaid Thanawarothon, Paripat Pairat, Christophe Bouvet, Laurent Mezeix

Composites: Mechanics, Computations, Applications: An International Journal 9(2):1–17 (2018)

NONCIRCULAR CFRP BICYCLE'S CHAINRING. PART I: STATIC AND LOW-VELOCITY IMPACT ANALYSIS

Zhorachaid Thanawarothon,[1] Paripat Pairat,[2] Christophe Bouvet,[3] & Laurent Mezeix[1,*]

[1]*Faculty of Engineering, Burapha University, 169 Long-Hard Bangsaen Road Chonburi 20131, Thailand*

[2]*Geo-Informatics and Space Technology Development Agency, Space Krenovation Park (SKP) 88 Moo 9, Thungsukhla, Sriracha, Chonburi 20230, Thailand*

[3]*Université de Toulouse, INSA, UPS, Mines d'Albi, ISAE, ICA (Institut Clément Ader), 135 Avenue de Rangueil, 31077 Toulouse Cedex, France*

*Address all correspondence to: Laurent Mezeix, Faculty of Engineering, Burapha University, 169 Long-Hard Bangsaen Road Chonburi 20131, Thailand, E-mail: Laurent.mezeix@hotmail.com

The paper presents an experimental analysis to determine the teeth failure of noncircular composite chainring. A noncircular carbon/epoxy chainring with a specific stacking of 11 plies is studied. In a first step, a quasi-static tensile test is realized on the chain and on the chainring to determine their strength. As the damage of composites is a major concern, as a second step the low-velocity/low-energy impact drop tests are performed. Five levels of impact energy are investigated in order to study the energy effect on the teeth damage, and the damage localization is analyzed using C-Scan. Quasi-static results show that the metallic chain fails first. Experimental impact results reveal that teeth damage is presented only for an impact higher than 1.6 J. Finally, the total teeth failure appears for an energy close to 2.5 J.

KEY WORDS: *noncircular chainring, CFRP, failure, experiments, low-velocity impact*

1. INTRODUCTION

The usage of Carbon Fiber Reinforced Polymers (CFRP) within the aerospace, structural engineering, land transports, and sport industries have increased significantly over the past 40 years. Due to their high modulus and strength and their low density, gain of mass is expected. Although CFRP present better mechanical

properties than aluminum, impact (Bouvet and Rivallant, 2016; Rozylo et al., 2017) and edge damage (Ostré et al., 2016; Li and Chen, 2016) are a major concern. Indeed, a large damage inside the laminate of composite structure is created by low-velocity/low-energy impact, while indentation is barely visible on its surface. Actually, during the lifecycle of a composite structure, such impacts happen, generally, due to the maintenance tool drop or in-service debris impact. A large number of researches proved that low-velocity/low-energy impact produces a complex internal damage, and it can be catalogued as: delamination, matrix cracking, and fiber rupture (Abrate, 2005; Hongkarnjanakul and Bouvet, 2013). The CFRP strength can be considerably reduced after a low-velocity impact, especially its compressive strength (Cantwell and Morton, 1991). A decrease of about 25% in the ultimate tensile strength was observed after an impact energy of 6.8 J (Mosallam et al. 2008). Therefore, the governing mechanisms related to the precipitate composite structure failure need to be understood in order to improve its residual strength.

Many sports take advantage of composites to increase the specific strength of the equipment. CFRP replace wood for tennis racquets and baseball bats (Brody, 1997) and replace steel for golf clubs to reduce the weight and to increase the ball exit velocity (Slater et al. 2010). Boardsports as snowboarding, surfing or skateboarding take advantage of composite material to increase the bending and torsion stiffness of the board (Clifton et al., 2010). CFRP are largely used in competition cycling especially for the frame to obtain a high stiffness and strength structure at low weights (Jin-Chee and Wu, 2010). Experiments show that the mountain bikes are impacted by stones with an energy lower than 3 mJ (Höchtl et al., 2012). Chainring can be manufactured of either an aluminum alloy or CFRP (Fig. 1a) and can be circular or not (Bini and Dagoese, 2012). Indeed, the average crank power output can be increased by using noncircular chainrings (Rankin and Neptune, 2008). B. Wiggins won the Tour de France in 2011 with a metallic oval rings and C. Froome with an osymetric chainrings since 2013[**Q2**]. However, the noncircular carbon composite chainring is not yet habitually used. Indeed, a noncircular carbon woven/epoxy chainring with a thickness of 2.5 mm had shown teeth failure during professional cycling. Moreover, the teeth failure always appears in the same place (Fig. 1a). Two types of failure were observed (Fig. 1b), teeth breaking through its cross section (1) and plies snatching (2).

To the best of our knowledge, teeth failure of composite chainring has not been investigated in detail as yet. Therefore, in this paper, experimental analysis has been performed in order to analyze the teeth failure mechanism of noncircular composite chainring. Dedicated quasi-static and low-velocity impact experiments have been firstly designed. Then, quasi-static tests of the chain and of the noncircular composite chainring are carried out to determine their strength. Finally, low-velocity impact drop tests and Non Destructive Testing (NDT) are performed in order to study the energy level necessary to damage the chainring teeth.

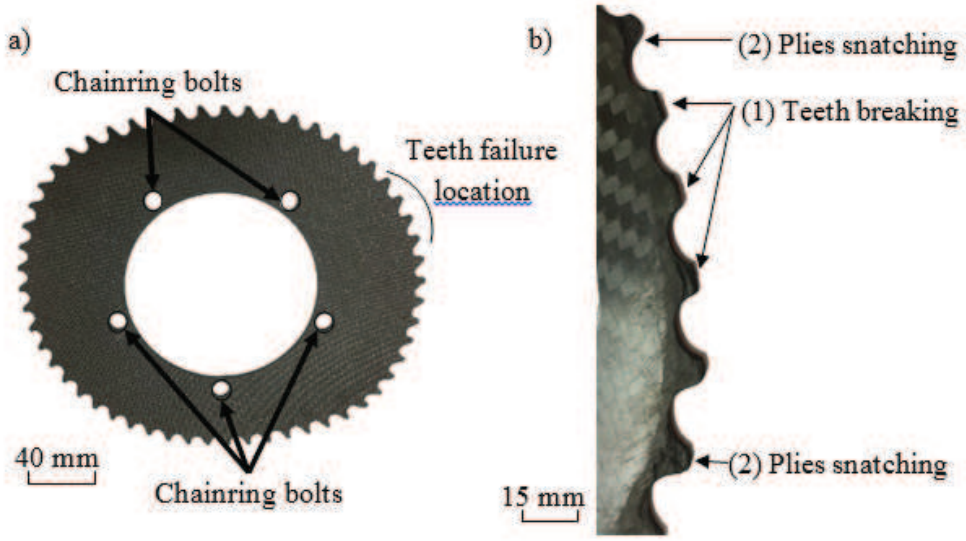

FIG. 1: Typical shape (a) and teeth failure (b) of noncircular CFRP chainring

2. CASE STUDY AND EXPERIMENTAL STUDY

2.1 Chainring and Chain

Noncircular composite chainring with 53 teeth are studied in this paper (Fig. 2). The radius of the noncircular chainring depended on the angle θ (Table 1). The teeth de-

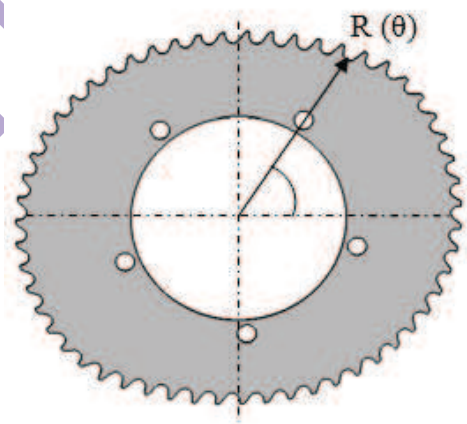

FIG. 2: Geometry of noncircular chainring

TABLE 1: Radius R of the noncircular chainring as a function of the angle θ

Angle, θ [°]	R [mm]
0	93.97
10	95.23
20	96.77
30	98.59
40	100.54
50	102.50
60	104.25
70	105.58
80	106.38
90	106.73
100	106.90
110	106.94
120	105.79
130	101.24
140	97.05
150	94.11
160	92.99
170	93.13
180	93.97

sign proposed by Wang is used in this research (Wang et al., 2016). The chain consisted of rollers, inner and outer plates (Fig. 3), and it is provided by SRAM (reference

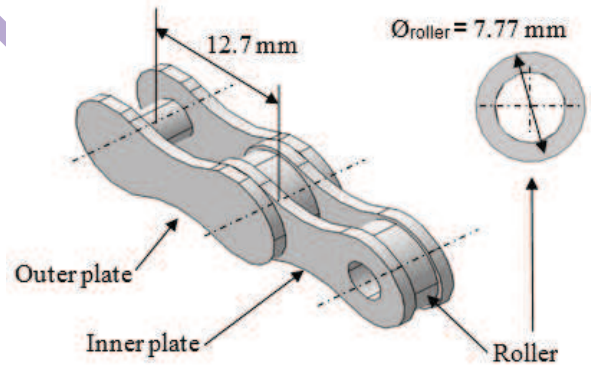

FIG. 3: Chain geometry

PC-991). Failure of the chain is noted for a force of 9000 N by the manufacturer (SRAM, 2018). Rollers diameter is 7.77 mm (0.306 in) and the chain pitch is 12.7 mm (0.5 in).

2.2 Materials and Manufacturing

The chain is made from steel (Table 2), while carbon 2/2 twill woven/epoxy is used for the chainring (Table 3). The chainring consists of 11 plies of 0.23 mm each with the following stacking: [30/60/0/60/30/0/30/60/0/60/30], given a chainring thickness of 2.53 mm after manufacturing. The chainring is manufactured through oven under 1 bar of pressure with a curing cycle of 80°C for 1 h followed by a hold step at 120°C during 3 h. Finally, teeth are cut thanks to a CNC with a carbide end mills — style 4 Flute (Ø 4 mm) and with a rotational speed of 15,000 rpm and a cutting speed of 5 mm/min (Fig. 4).

2.3 Tensile Test

The chain is firstly tested under tension in order to obtain its behavior and failure load. Seven pitches of the chain are studied corresponding to a length of 88.9 mm (Fig. 5). To determine the quasi-static mechanical behavior of the noncircular composite chairing, a specific bench is designed (Fig. 6). The chainring is clamped between two metallic plates thanks to 5 bolts, and the bench is fixed to the lower table

TABLE 2: HSS steel (Azo Materials, 2012)

Material	E [GPa]	η	σ_y [MPa]	ρ [kg/m^3]
Steel AISI 4140	210	0.30	415	7900

TABLE 3: Carbon 2/2 twill woven/epoxy ply properties

Carbon 2/2 twill woven/epoxy ply (T300/EPOTEC YD 535 LV, TH 7253 — 8)	
Longitudinal Young's modulus, E_l	35 GPa
Transverse Young's modulus, E_t	35 GPa
Shear modulus, G_{lt}	4.3 GPa
Poisson's ratio	0.05
ρ [kg/m^3]	1700
Failure	
Longitudinal tensile strength, $\sigma_l^{f,t}$	800 MPa
Transverse tensile strength, $\sigma_t^{f,t}$	800 MPa
In-plane shear strength, τ_{lt}^{f}	98 MPa
Out-of-plane shear strength, τ_{tz}^{f}	50 MPa

FIG. 4: Teeth cutting process on typical carbon/epoxy chainring

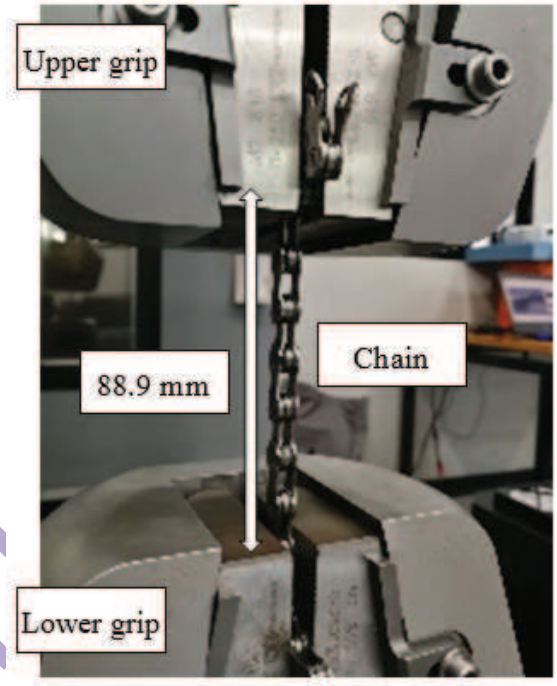

FIG. 5: Chain tensile test

of the tensile machine. The noncircular chainring position is chosen in such a way that the broken teeth observed on the part used in the bike were tested (Fig. 1). The chain is then installed and the free extremity is pulled thanks to the upper grip of the tensile machine. A pretension of 50 N is firstly applied in order to assure the position of the chain with the chainring. For both chain and chainring, a constant velocity of 0.5 mm/min is used, and the force and displacement are tracked during the test with an acquisition rate of 10 acq/s.

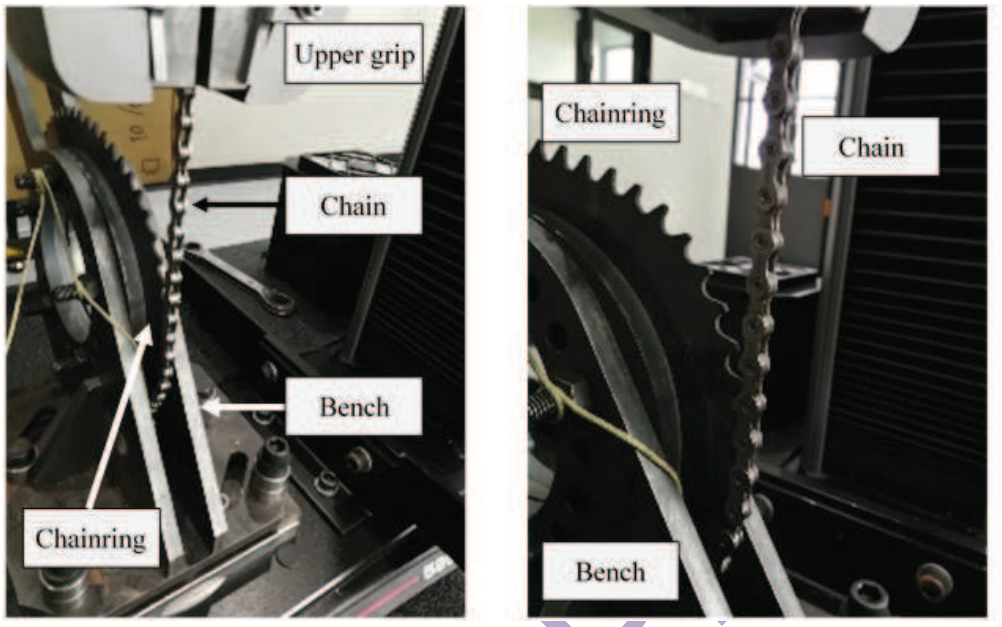

FIG. 6: Chainring tensile test

2.4 Low-Velocity/Low-Energy Impact Test

Composite chainring can be subjected to impact from two main origins. Firstly, during off-road biking the chainring can be hit by stones and the maximum energy of such impact was experimentally measured at 2.43 mJ (Höchtl et al., 2012). Secondly, during the storage or maintenance of the chainring, hand tool or other objects can be dropped, and the chainring can be impacted. To represent such impacts, tests are performed on a drop weight testing rig with a hemispherical shape indentor of 8-mm diameter (Fig. 6). A mass of 0.585 kg is attached to the impactor. The impact located on the teeth is the most dramatic location as the damage could reduce their strength and so decrease the composite chainring final failure load. Therefore, a low-velocity impact test is performed at the centre of the teeth and to avoid influence of other impact tests, only one tooth of three is impacted (Fig. 7)[**Q1**]. Moreover, as quasi-isotropic stacking is used, the noncircular shape has no influence on the impact results. The chainring is clamped through 5 bolts on a lower circular support to represent the bicycle sprocket. To study the effect of the impact energy on the teeth damage, five levels of energy are used: 0.5 J, 1 J, 1.5 J, 2 J, and 3 J. The contact force is measured with a piezoelectric sensor during the test. Moreover, the initial impact velocity is obtained from an optical sensor. After impact, delamination is measured with a C-Scan system provided by the TESTIA company.

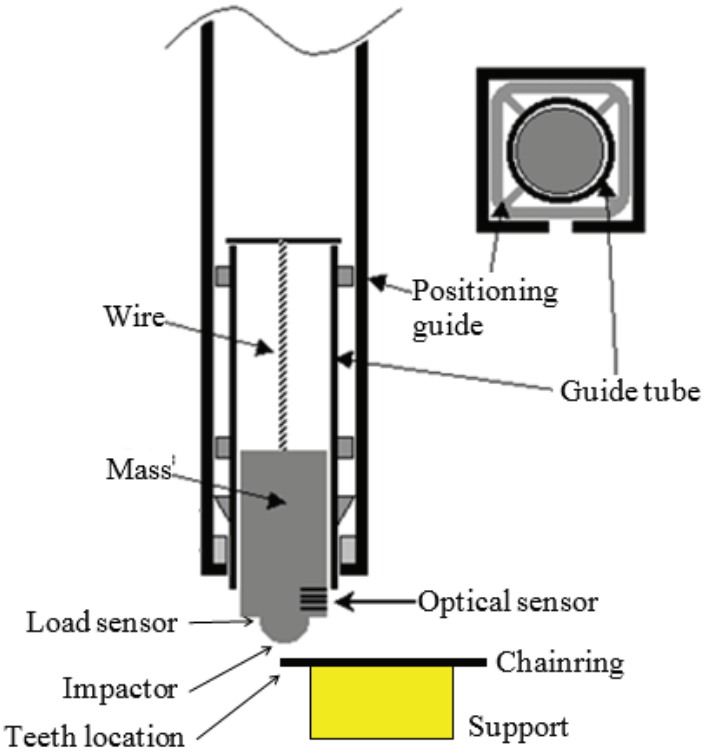

FIG. 7: Impact test design

3. EXPERIMENTAL RESULTS

3.1 Chain Behavior

Firstly, the chain has been tested in order to verify its failure load (Fig. 9). The force–displacement curve consists in a first by the linear behavior until 4000 N (1)[**Q3**]. Then, the plasticity of the metallic chain starts and propagates (2) until the final fail at a load of 9200 N (3), as given by the manufacturer (26) [**Q4**].

3.2 Quasi-Static Tensile of Noncircular Composite Chainring

Two noncircular composite chainrings are tested. The force–displacement curve consists of three steps (Fig. 10). Firstly, linear behavior (1) is observed until a force of 4500 N (2) that corresponds to the beginning of the chain damage (Fig. 9). Then, the damage of the chain propagates (3) until the failure of the chain that happens for a load of 8100 N and 9100 N (4). Therefore, the observed failure of noncircular composite chainring is certainly due to the impact damage.

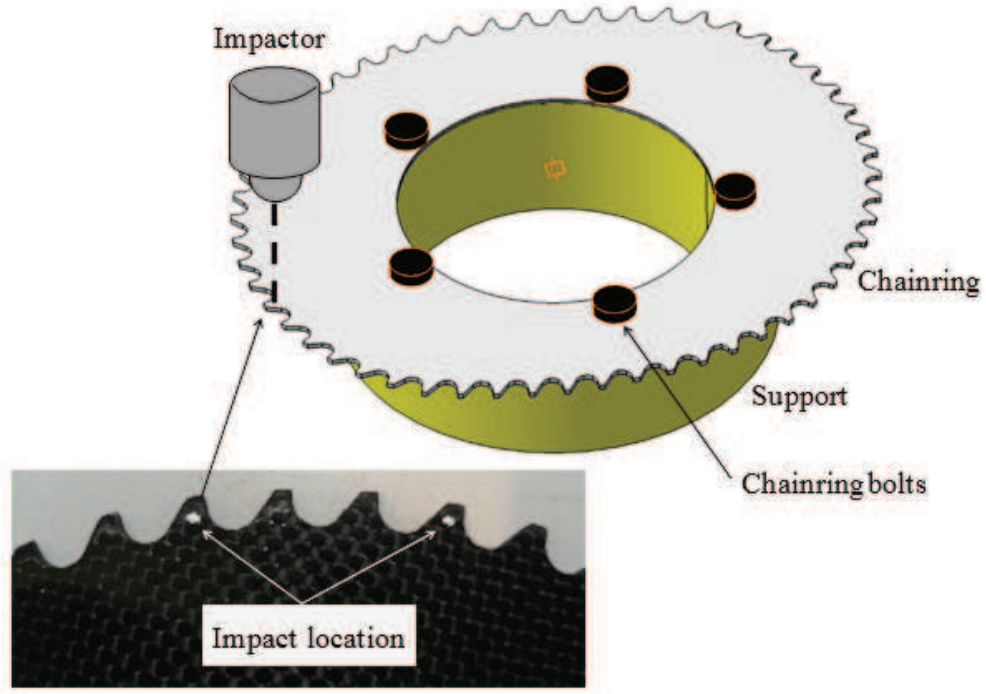

FIG. 8: Chainring impact test design

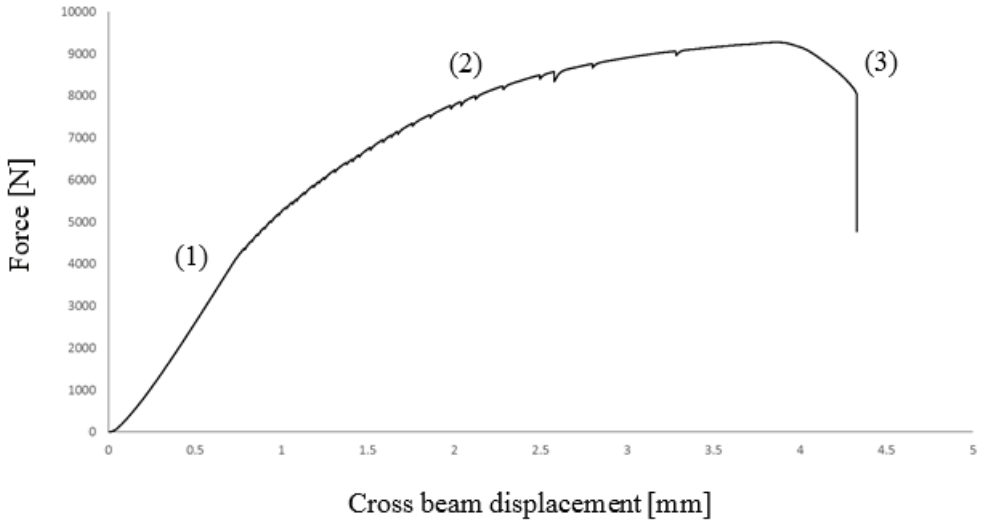

FIG. 9: Force–displacement of the chain

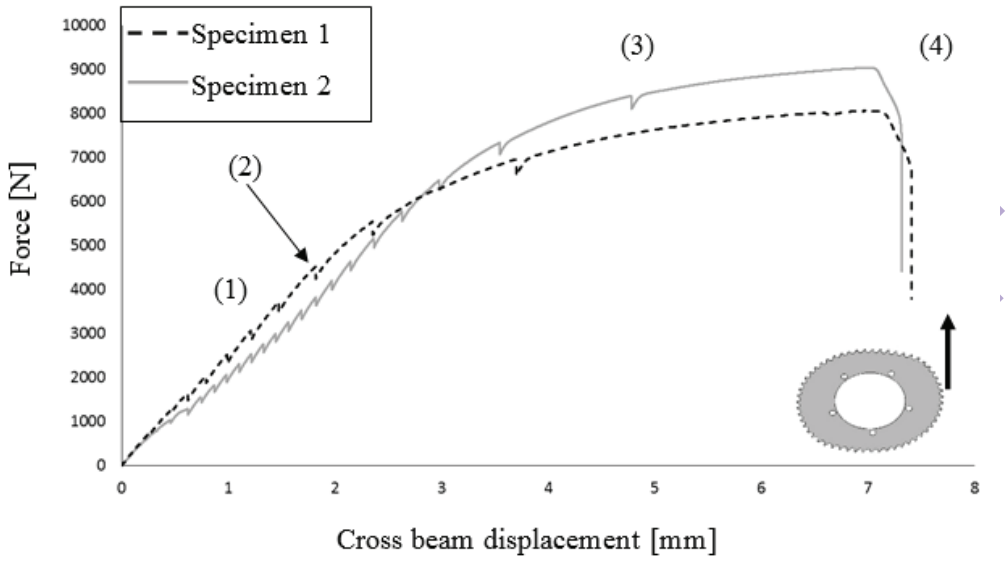

FIG. 10: Force–displacement of the composite noncircular chainring

3.3 Low-Velocity Impact Tooth Behavior

Figures 11 to 14 show the impact force–displacement curves of the noncircular composite chainring. Except for impacts of 2 J and 3 J, three impact tests are performed, and the results show that they are quite reproducible (Figs. 11–13). Two tests are carried out for an impact of 2 J and only one for 3 J (Fig. 14). One of the 2 J tests shows tooth break, while for the highest impact energy, the tooth failure was observed. Finally, the tooth should totally fail for an impact energy close to 2.5 J.

The force–displacement curves of the five different impact energies are plotted in Fig. 15 for comparison. Specimen's curves are very similar to the respective corresponding impact energy. The impact phases, from the damage mechanism point of view, are reflected in the changes of the force–displacement curve. Three major phases can be distinguished. Firstly, the force increases linearly with the same slope (1) corresponding to the initial teeth stiffness. According to the force curves, the onset of important damage is at around 0.58 kN (2). Moreover, damage is only observed for energy higher than 1.5 J. For specimens impacted with an energy of 1.5 J, 2 J, and 3 J, the second phase of the impact is characterized by the damage propagation, and it is determined by a stable force (3). Finally, except for the impact of 3 J, which presents tooth failure (Fig. 14), the impactor rebounds, and so the force and displacement decrease (4). For the impact energy 0.5 J and 1 J the displacement comes back to the initial position, while for a higher energy residual displacement is observed (5). This difference between the initial and final position corresponds to the residual indentation characterizing teeth damage (Table 3).

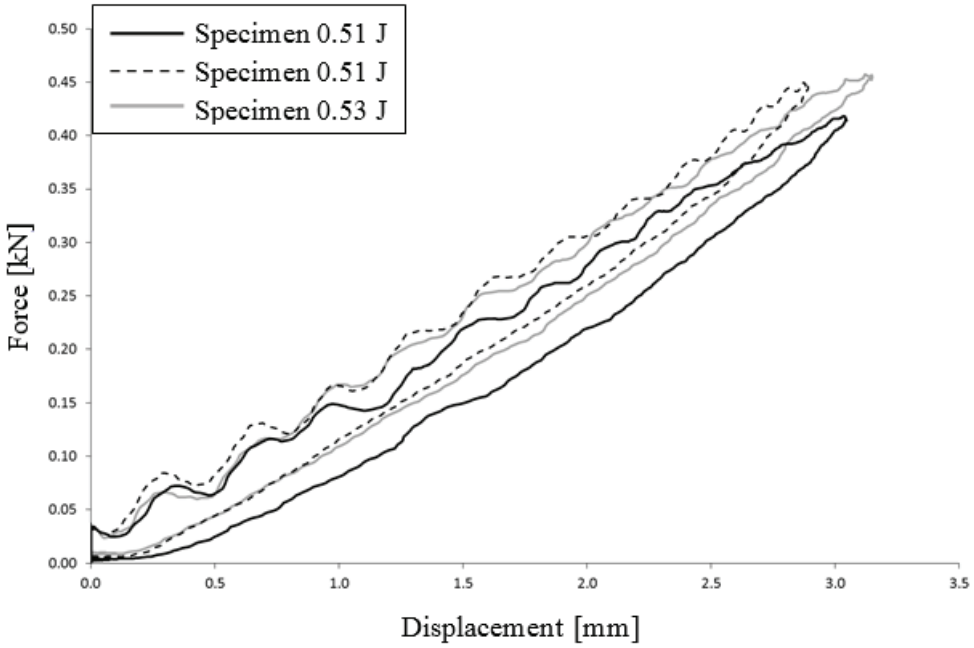

FIG. 11: Evolution of force–displacement curves for an impact of 0.5 J

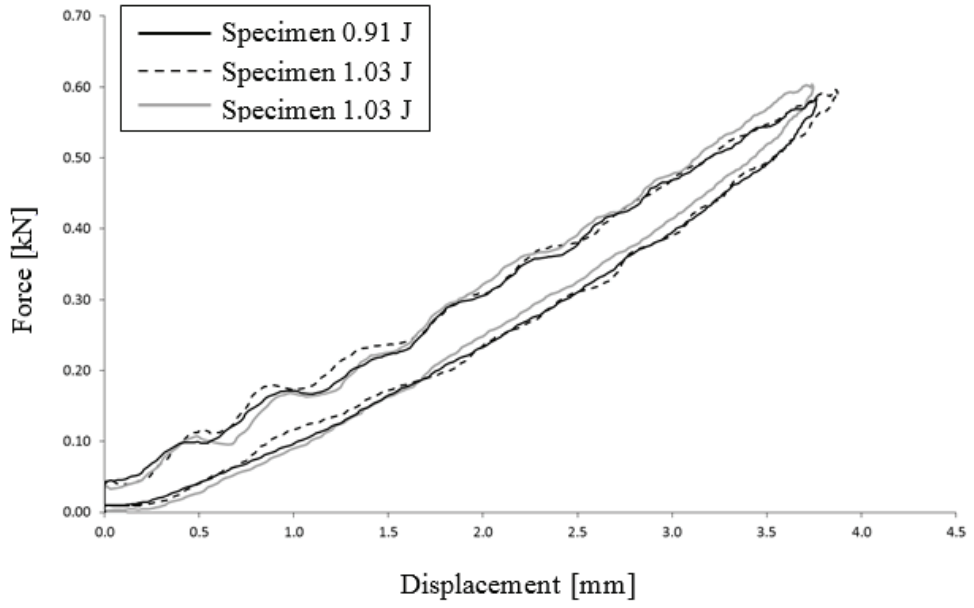

FIG. 12: Evolution of force–displacement curves for an impact of 1.0 J

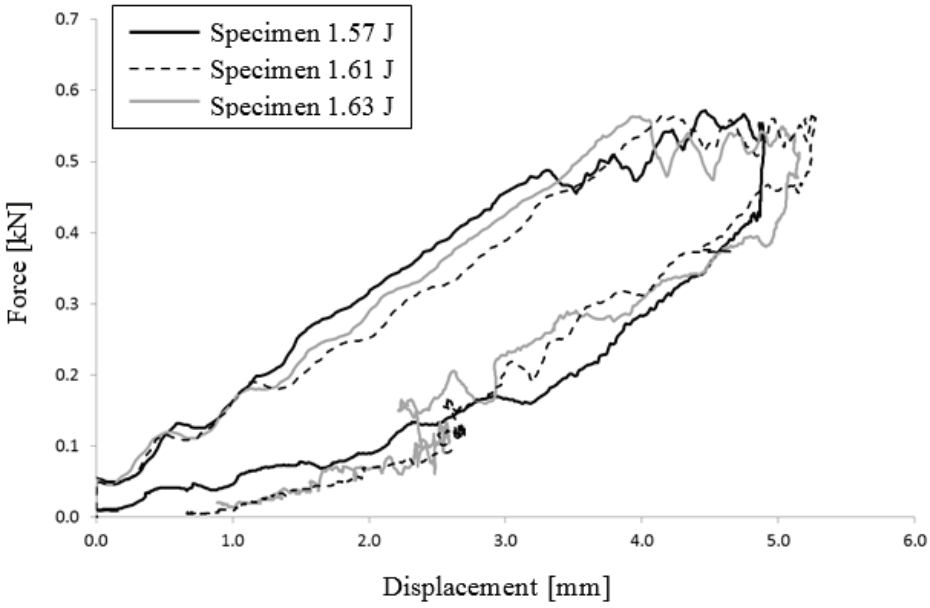

FIG. 13: Evolution of force–displacement curves for an impact of 1.5 J

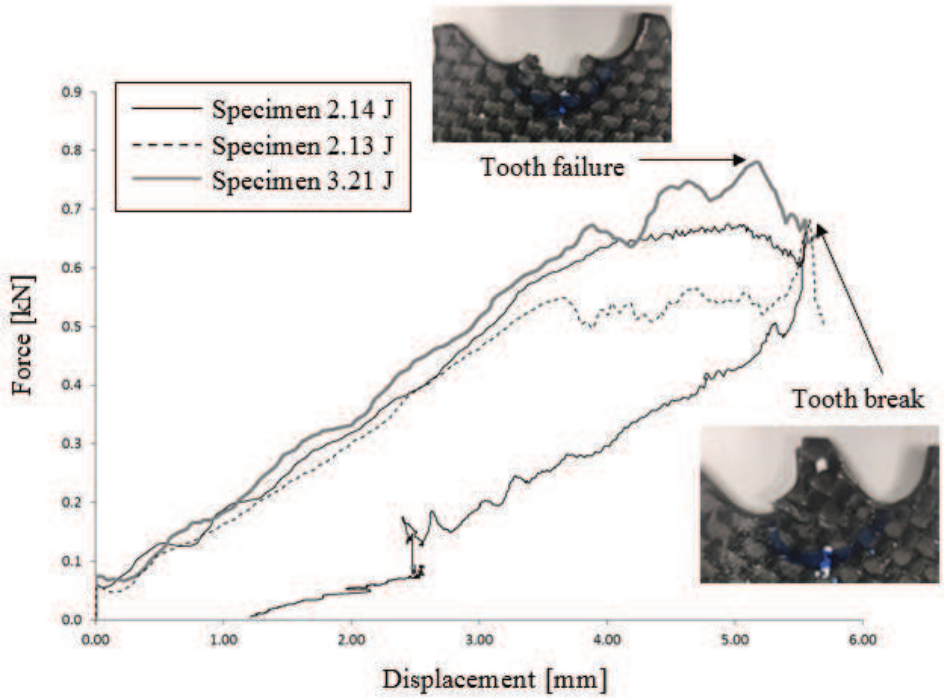

FIG. 14: Evolution of force–displacement curves for an impact of 2.0 and 3.0 J

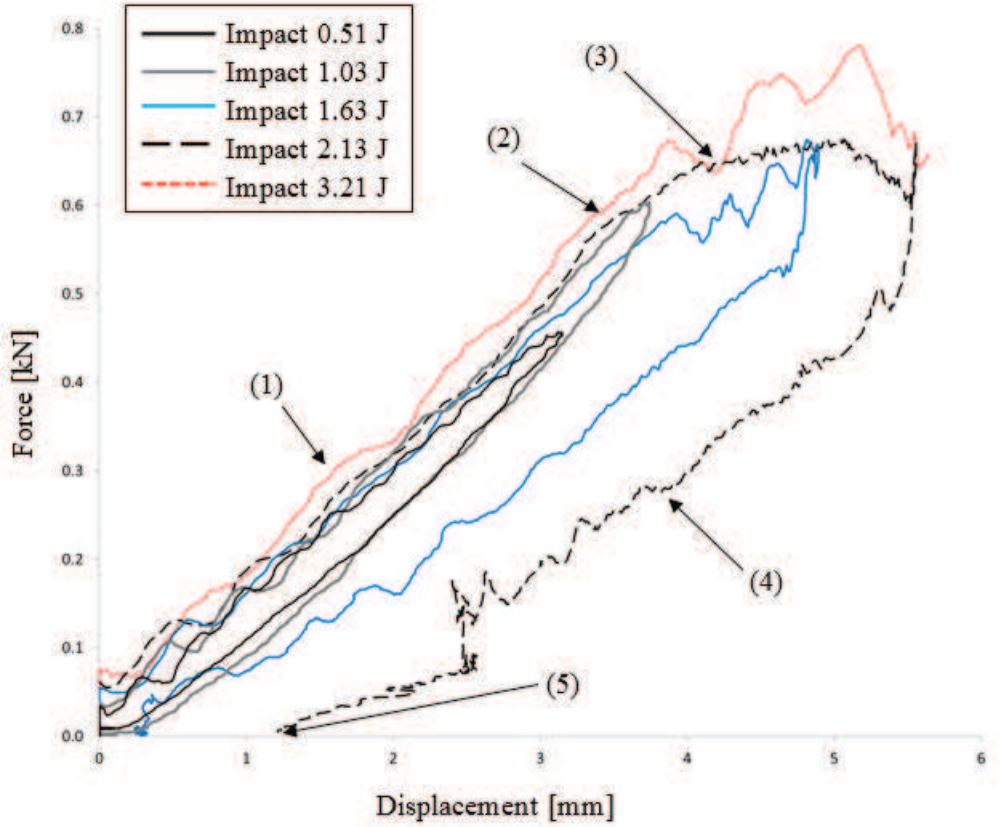

FIG. 15: Force–displacement of the composite noncircular chainring

A Non Destructive Test (NDT) of an ultrasonic system is widely used for identifying the impact damage in CFRP laminates. It can provide information regarding both the damage area and thickness localization of material discontinuities like the debonding of interfaces. C-Scan is performed from the impacted face of the noncircular composite chainring thanks to Phased Array Probe 64 elements 5 MHz from TESTIA (Fig. 16). A summary of the impact results is presented in Table 4. For each test, data is presented in terms of: the maximum filtered impact force during the test and the residual indentation. Also provided is the projected delamination size area obtained. Firstly, for an impact energy lower than 1.57 J no delaminations are noted that would confirm observations made from the force–displacement curves (Figs. 11 and 12), while first damages are observed for 1.61 J and 1.63 J. Thus, the first damage should appear for an energy impact of about 1.6 J. Moreover, the C-Scan shows that the delamination are located between the ply 4 and 6 (Fig. 17). As the energy increases, larger delamination is observed, in particular, the length expanding largely until the attainment of a maximum of 15 mm for an impact energy of 2.13 J. Contrariwise, the

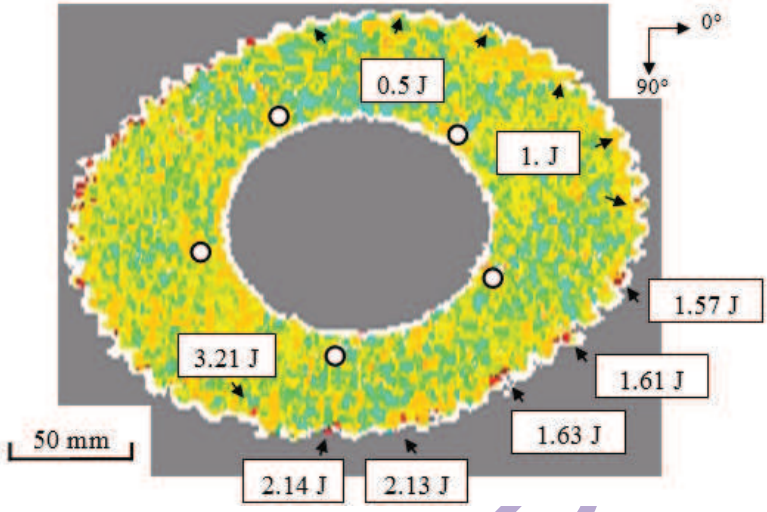

FIG. 16: C-Scan from the impacted side of noncircular composite chainring of specimen impacted at 0.5 J, 1 J, 1.5 J, 2 J, and 3 J

TABLE 4: Summary of the impact results

Impact energy [J]	Peak Force [kN]	Residual Indentation [mm]	Damage Length [mm]	Damage Width [mm]	Through Thickness Damage Location [mm]
0.51	0.42	—	—	—	—
0.51	0.46	—	—	—	—
0.53	0.45	—	—	—	—
0.91	0.60	—	—	—	—
1.03	0.59	—	—	—	—
1.03	0.60	—	—	—	—
1.57	0.55	—	—	—	—
1.61	0.56	0.70	10	9	0.96–1.10
1.63	0.56	0.97	12	8	0.96–1.09
2.13	0.68	1.24	15	10	0.95–1.30
2.14	0.68	Tooth break	11	11	0.90–1.82
3.21	0.78	Tooth failure	15	11	> 0.94

width is less influenced by the impact energy. Moreover, higher is the impact energy, deeper is the delamination location. For an impact energy of 2.13 J delaminations are located between the ply 4 and 6 and for 2.14 J between the ply 4 and 9 (Fig. 17).

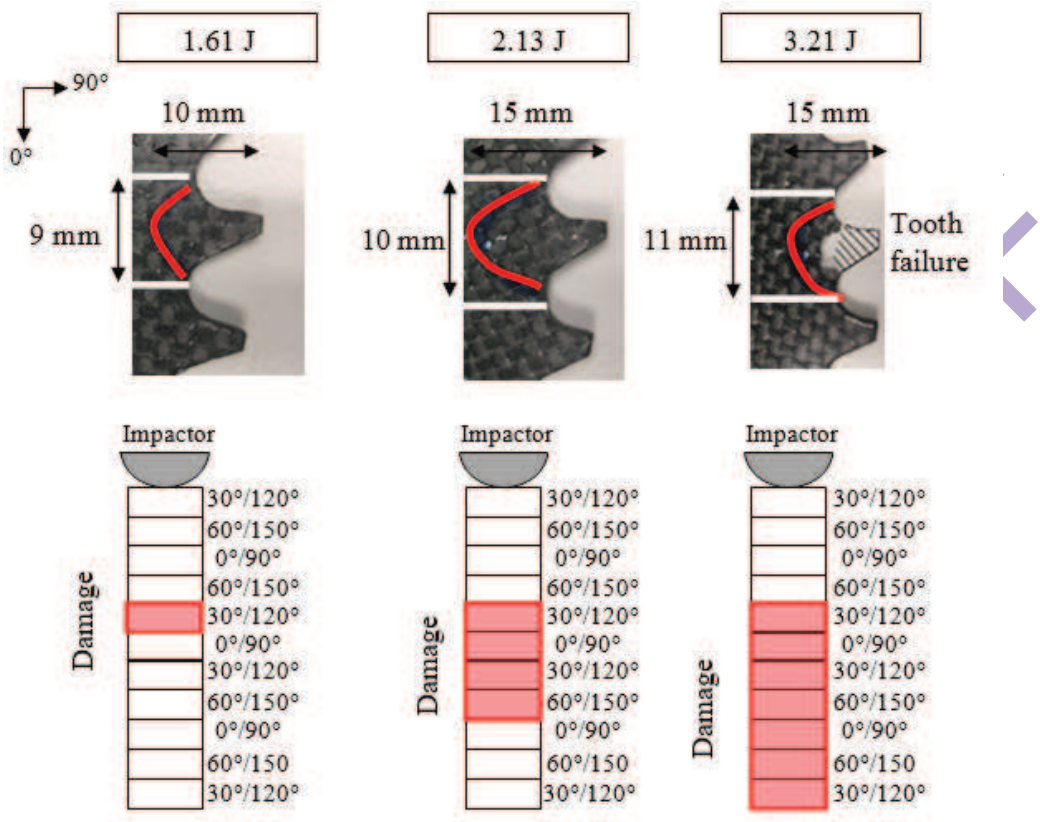

FIG. 17: Details of delamination location of specimen impacted at 1.61 J, 2.13 J, and 3.21 J

4. CONCLUSIONS

Noncircular composite chainring exhibits teeth failure during professional cycling. Moreover, failures appear always at the same location. In order to optimize the design, failure mechanisms has to be investigated. CFRP made of 11 plies with a quasi-isotropic stacking, [30/60/0/60/30/0/30/60/0/60/30], of carbon woven/epoxy were studied. Firstly, quasi-static tests were performed, and the results showed that the composite chainring does not fail. Indeed, the metallic chain firstly broke at a load of about 9000 N. However, CFRP damage is a major concern and therefore, low-velocity impact drop tests were performed with 5 levels of energy. Results showed that for an energy lower than 1.6 J laminate does not presented damage. This energy corresponds to the fall from a workbench of 0.8 m height of an object of 200 g. For higher energy, no damage were visible on both surfaces due to their location inside the chainring. Indeed, C-Scan confirmed the presence of delamination between ply 4 and 8. Finally, teeth failed for an impact close to 2.5 J.

Teeth breaking and ply snatching observed on specimen are potentially due to the impact of the chain on the chainring. Indeed, when a cyclist shifts the gear, the chain can impact chainring teeth and, in the case of CFRP part, could damage it reducing its strength. Consequently, in order to design the chainring in such a way that the potential damage is taken into account a damage tolerance validation is necessary to be determined by performing a tensile test on a impacted composite chainring. The residual strength of damaged composite chainring is currently in progress to determine the influence of the delamination on the chainring strength. Moreover, numerical simulation is also under investigation in order to optimize the tooth design.

ACKNOWLEDGMENTS

The authors wish to thank the Geo-Informatics and Space Technology Development Agency (GISTDA) for its support in manufacturing and testing operations. The authors gratefully acknowledge TESTIA ASIA PACIFIC for their support in the C-Scan operations.

REFERENCES

Abrate, S., *Impact on Composite Structures*, Cambridge University Press, 2005.

Azo Materials, http://www.azom.com/, 2012.

Bini, R.R. and Dagoese, F., Noncircular Chainrings and Pedal to Crank Interface in Cycling: A Literature Review, *Braz. J. Kinantropom. Hum. Perform.*, vol. **14**, pp. 470–482, 2012.

Bouvet, C. and Rivallant, S., Damage Tolerance of Composite Structures under Low-Velocity Impact, in: V. Silberschmidt, Ed., *Dynamic Deformation, Damage and Fracture in Composite Matererials and Structures*, Woodhead Publishing, pp. 7–33, 2016.

Brody, H., The Physics of Tennis. III: The Ball–Racket Interaction, *Am. J. Phys.*, vol. **65**, pp. 981–987, 1997.

Cantwell, W. and Morton, J., The Impact Resistance of Composite Materials — A Review, *Compos.*, vol. **22**, pp. 347–362, 1991.

Clifton, P., Subic, A., and Mouritz, A., Snowboard Stiffness Prediction Model for Any Composite Sandwich Construction, *Proced. Eng.*, vol. **2**, pp. 3163–3169, 2010.

Höchtl, F., Hein, M., Klug, S., and Sennera, V., On the Effect of Chain Stay Impact on the Structural Safety of CFRP Structures in Mountain Biking, *Proced. Eng.*, vol. **34**, pp. 664–669, 2012.

Hongkarnjanakul, N. and Bouvet, C., Validation of Low Velocity Impact Modeling on Different Stacking Sequences of CFRP Laminates and Influence of Fiber Failure, *Compos. Struct.*, vol. **106**, pp. 549–559, 2013.

Jin-Chee Liu, T. and Wu, H.C., Fiber Direction and Stacking Sequence Design for Bicycle Frame made of Carbon/Epoxy Composite Laminate, *Mater. Des.*, vol. **31**, pp. 1971–1980, 2010.

Li, N. and Chen, P.H., Experimental Investigation on Edge Impact Damage and Compression-After-Impact (CAI) Behavior of Stiffened Composite Panels, *Compos. Struct.*, vol. **138**, pp. 134–150, 2016.

Martin, J.C., Lamb, S.M., and Brown, N.A., Pedal Trajectory Alters Maximal Single-Leg Cycling Power, *Med. Sci. Sports Exerc.*, vol. **34**, pp. 1332–1336, 2002.

Mosallam, A., Slenk, J., and Kreiner, J., Assessment of Residual Tensile Strength of Carbon/Epoxy Composites subjected to Low-Energy Impact, *J. Aerospace Eng.*, vol. **21**, pp. 249–258, 2008.

Ostré, B., Bouvet, C., Minot, C., and Aboissière, J., Finite Element Analysis of CFRP Laminates subjected to Compression after Edge Impact, *Compos. Struct.*, vol. **153**, pp. 478–489, 2016.

Rankin, J.W. and Neptune, R.R., A Theoretical Analysis of an Optimal Chainring Shape to Maximize Crank Power during Isokinetic Pedaling, *J. Biomech.*, vol. **41**, pp. 1494–1502, 2012.

Rozylo, P., Debski, H., and Kubiak, T., A Model of Low-Velocity Impact Damage of Composite Plates subjected to Compression-After-Impact (CAI) Testing, *Compos. Struct.*, vol. **181**, pp. 158–170, 2017.

Slater, C., Otto, S.R., and Strangwood, M., The Quasi-Static and Dynamic Testing of Damping in Golf Clubs Shafts Fabricated from Carbon Fibre Composites, *Proced. Eng.*, vol. **2**, pp. 3361–3366, 2010.

SRAM, PC-991 Chain. https://www.sram.com, 2018.

Wang, Y., Ji, D., and Zhan, K., Modified Sprocket Tooth Profile of Roller Chain Drives, *Mech. Theor.*, vol. **70**, pp. 380–393, 2013.

[Q1] AU: Please check. Figure 8 is not mentioned in the text. Please indicate its place
[Q2], [Q3] AU: Please check the sense of the sentence. It is not clear
[Q4] AU: Please check. What does this figure means?